Search for isotope effects in projectile and target ionization in swift He^+ on H_2 or D_2 collisions

F. Trinter,* M. Waitz, M. S. Schöffler, H.-K. Kim, J. Titze, O. Jagutzki, A. Czasch, L. Ph. H. Schmidt, H. Schmidt-Böcking, and R. Dörner

Institut für Kernphysik, Goethe-Universität Frankfurt am Main, 60438 Frankfurt, Germany

(Received 11 November 2013; published 6 March 2014)

Using the cold target recoil ion momentum spectroscopy (COLTRIMS) technique, we have measured the simultaneous projectile and target ionization in collisions of He^+ projectiles with a mixture of gaseous H_2 and D_2 for an incident projectile energy of 650 keV. Motivated by Cooper *et al.* [Phys. Rev. Lett. **100**, 043204 (2008)], we look for differences in the ionization cross section of the two isotopes with the highest resolution and statistical significance. Contributions of the electron-electron and electron-nucleus interactions have been clearly separated kinematically by measuring the longitudinal and transverse momentum of the recoiling ion. We find no significant isotope effect in any of our momentum distributions.

DOI: 10.1103/PhysRevA.89.032702 PACS number(s): 34.50.Gb, 33.15.Ry, 34.80.Gs

I. INTRODUCTION

On the atomic scale, interaction such as photoionization and charged particle impact is completely dominated by the electromagnetic force. If one neglects the tiny hyperfine structure splitting, the nucleus just provides the Coulomb potential in which the electrons move. The ionization of single atoms by charged particles is therefore not expected to depend on the isotope. Because the chemical behavior of an atom is largely determined by its electronic structure, different isotopes also exhibit very similar chemical behavior. The main exception to this is the kinetic isotope effect: due to their larger masses, heavier isotopes tend to react slightly more slowly than lighter isotopes of the same element. This effect is most pronounced for H and D, because deuterium has twice the mass of the proton. The mass effect between H and D also affects the behavior of their respective chemical bonds by changing the center of gravity (reduced mass) of the atomic system [1,2]. For heavier elements, the mass-difference effects on chemistry are usually negligible. In general, absolute and differential cross sections for ionization by fast charged particles are believed to be isotope-independent.

In surprising contrast, Cooper and co-workers observed differences in quasielastic (energy transfer is small compared to the incident energy of the scattered particles) electron-scattering cross sections from gaseous H_2, D_2, and HD molecules [3]. Electron scattering with a relatively high momentum transfer was measured, and experimentally determined cross sections were compared with calculated ones using Rutherford scattering theory, where the scattering cross sections depend only on the charge and not on the mass of the target. Cooper *et al.* found, however, that the ratio $I(\mathrm{H})/I(\mathrm{D})$ of the scattering intensities showed a much smaller value than expected from this conventional theory. For a 50:50 H_2-D_2 gas mixture, they found a ratio of the respective scattering intensities of $\approx$0.7 (a shortfall of $\approx$30%), while for the HD gas $\approx$1 has been seen, as expected. Following these results, the absolute elastic scattering probability for H_2 and the appropriate geometrical cross section seem to be smaller than expected. On the other hand, the ratio of the electron scattering intensities of H and D in the case of the HD gas agrees well with the predictions of Rutherford scattering.

Cooper *et al.* [3] speculated that entanglement between identical nuclei (in H_2 and D_2) could play a crucial role. They argued that possibly short-time entanglement of the protons with their adjacent electrons and nuclei might reduce the cross section. With this speculation, they challenged the common independent scatterer model. They assumed that for fast, large momentum transfer electron scattering on a very short time scale, the H_2 wave function cannot be separated to a product of a single-particle wave function for electrons and nuclei, and that the scattering is not effectively the sum of the scattering at any of these isolated particles. The entangled scatterer could lead to a smaller cross section in contrast to conventional theory. Then the lifetime of these quantum entanglements could be measured indirectly. They estimate that their scattering processes correspond to typical scattering times of about 500 attoseconds. If the entanglement between neighboring particles is responsible for the anomaly in the cross sections, the lifetime of the entanglement must be much longer than the scattering time. In this case, the lifetime of the entanglement could be probed by varying the momentum transfer and therefore the scattering time.

Related anomalies in the cross sections of hydrogen have been observed for different scattering systems: neutron scattering from H_2O and D_2O molecules [4], electron and neutron scattering from solid polymers [5], and neutron scattering from molecular hydrogen [6]. All these results represent a challenge for conventional scattering theory as well as for molecular spectroscopy. As of yet, no quantitative theory can explain all these anomalies, but all the suggested approaches today contain quantum entanglement [6–11]. There is also criticism of the measurements by Cooper *et al.*; see [12], and references therein. Moreh suspects that the origin of the above deviations is instrumental and not due to any real deviation from the Rutherford formula. He argues that the heavier gas component in any binary gas mixture from an inlet spends on average more time in the interaction region, which would cause the observed anomaly.

To shine more light on these unexpected experimental findings in electron and neutron scattering, we use a different

*trinter@atom.uni-frankfurt.de

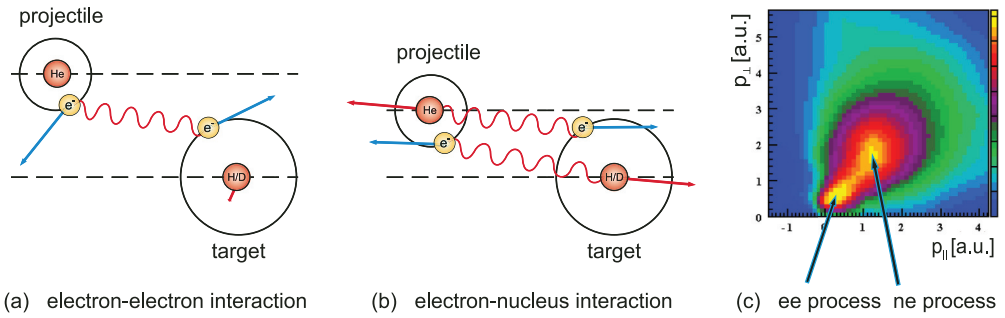

FIG. 1. (Color online) Cold target recoil ion momentum spectroscopy (COLTRIMS) allows us to separate experimentally the contribution of the *ee* interaction from the *ne* interaction to the ionization of the projectile, as shown in the doubly differential cross section $d^2\sigma/(dp_\parallel dp_\perp)$. For illustration, part (c) shows the recoil ion momentum distribution for a collision of $He^+ + He \rightarrow He^{2+} + He^+ + 2e^-$ at 1 MeV, the horizontal axis shows the longitudinal recoil ion momentum (parallel to the projectile beam direction), and the vertical axis shows the transverse recoil ion momentum (perpendicular to the projectile beam direction).

approach here. We investigate the following reactions:

$$He^+ + H_2 \rightarrow He^{2+} + {H_2}^+ + 2e^-, \quad (1)$$

$$He^+ + D_2 \rightarrow He^{2+} + {D_2}^+ + 2e^-. \quad (2)$$

In this process, simultaneously one electron is ejected from the target (H_2 or D_2) and one from the projectile (He^+). There are two mechanisms, termed *ee* and *ne*, which contribute to this reaction. In the *ee* process, the projectile electron is knocked out by an interaction with the target electron. This violent collision between two bound electrons leads to ejection of both of them from their respective binding. In the *ne* process, the projectile electron is ejected by an interaction with the target nucleus, and a second, independent interaction between the projectile nucleus and one of the target electrons facilitates the ejection of the target electron. Depending on the impact energy, one of these two processes dominates [13]. The *ee* process occurs at rather large impact parameters. The electrons knock each other out, while the nuclei are spectators in the reaction [see Fig. 1(a)]. Therefore, the overall momentum transfer to the target nucleus is small. A projectile velocity greater than 2 a.u. is needed to initiate the process. This threshold is due to the fact that the target electron, as seen from the projectile frame, must have sufficient kinetic energy that it can ionize the projectile and simultaneously escape from the target. For He, a projectile energy of 0.4 MeV is equivalent to an electron energy of 54 eV, which is the projectile binding energy [13,14]. For the *ne* process, on the contrary, the impact parameters are much smaller, leading to a larger transverse momentum transfer (perpendicular to the projectile beam direction), and in addition the longitudinal momentum (parallel to the projectile beam direction) is also compensated by the target nucleus [15]. Both electron loss processes are therefore separated in momentum space of the recoiling molecular hydrogen ion. Figure 1(c) shows the recoil ion momentum distribution for a collision of $He^+ + He \rightarrow He^{2+} + He^+ + 2e^-$ at 1 MeV. The most detailed investigations also measured the momenta of both electrons involved in the loss processes [16–18].

The key idea of our experiment is that the *ne* mechanism involves a violent scattering of the electron bound to the He^+ at the nucleus of H_2 or D_2, while the *ee* mechanism involves only the electrons. The 30% isotope differences in the scattering of free electrons at the nuclei reported in [3] might thus also affect the scattering of bound electrons in our collision system. The strength of our experiment is that the *ee* mechanism allows for robust *in situ* normalization of the data. While in any electron or neutron scattering experiment the comparison of cross sections for the different isotopes relies on the knowledge of the isotope ratio in the target gas mixture, this possible source of systematical error is not present in our experiment. The *ee* mechanism in our case is a scattering between the electrons; the nuclei are not active participants. Hence the previously reported isotope effects in electron and neutron scattering would not influence the *ee* contribution to the electron loss channel but only the *ne* contribution. We therefore search for differences in the *ne* versus *ee* contributions between the isotopes. While no standard scattering theory would predict such an isotope effect, the recent results of Cooper *et al.* on free-electron scattering would suggest such a difference of up to 30%.

II. EXPERIMENT

In our experiment, we use the cold target recoil ion momentum spectroscopy (COLTRIMS) technique [19–21] to examine the electron loss process [22–25] in collisions of He^+ projectiles with a gas mixture of 50% H_2 and 50% D_2. The He^+ ion beam is provided by the 2.5 MV Van de Graaff accelerator at the Institut für Kernphysik of Goethe Universität in Frankfurt. The beam is collimated using three sets of adjustable slits. In front of the reaction zone, an electrostatic deflector (beam cleaner) is used to separate the He^+ beam from charge state impurities (He^0 or He^{2+}). The reaction takes place in the overlap region of the He^+ beam with a supersonic gas jet providing the H_2 and D_2. An electric field projects the produced recoil ions (${H_2}^+$ or ${D_2}^+$) toward a time- and position-sensitive detector [26,27], yielding an acceptance angle of 4π for ions up to 5 a.u. momentum. Measuring the impact position on the detector and its time of flight, the particle trajectories and thus the particle momenta can be determined. To optimize the ion momentum resolution, an electrostatic lens is incorporated into the spectrometer system. Trajectory calculations including such lenses can be found in [28]. The diminishing influence of the extended interaction region on the momentum resolution can be strongly reduced by this focusing geometry. A drift tube following the acceleration part of the spectrometer yields

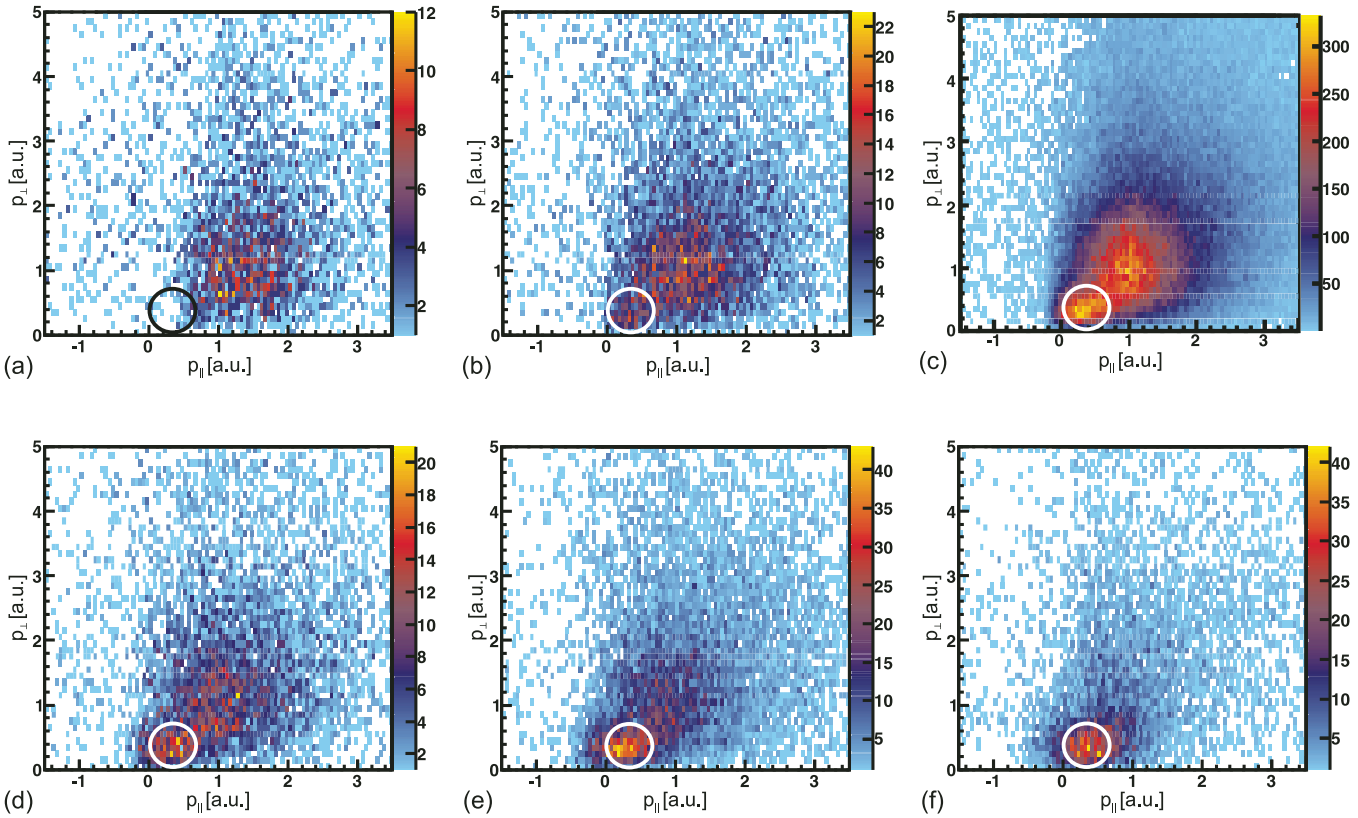

FIG. 2. (Color online) H_2^+ recoil ion momenta transverse and longitudinal to the incident beam direction for 400 keV (a), 550 keV (b), 650 keV (c), 700 keV (d), 900 keV (e), and 1500 keV (f) He^+ projectile energy [reaction (1)]. The *ee* process is marked by the circle.

focusing of the times of flight also in the third direction. The spectrometer has an electrical field of 6.5 V/cm and a length of 28 cm plus 150 cm recoil drift. Downstream of the spectrometer, another electrostatic deflector is used to charge-state-analyze the projectile beam after the reaction. He^+ projectiles are dumped in a Faraday cup, and only He^{2+} particles from the electron loss reaction are measured with a second position-sensitive detector. They serve as a trigger for our coincidence experiment. The data are acquired and stored in list mode format event-by-event. The typical times of flight were 12 μs for H_2^+ and 17 μs for D_2^+. The momentum resolution was determined by the simultaneously measured electron capture reaction $He^+ + H_2(D_2) \rightarrow He^0 + H_2^+(D_2^+)$ to be 0.1 a.u. Small fractions of false coincidences (<10%) were subtracted. The main source for this background is the single ionization with a wrongly detected projectile. In momentum space they are located around $p_\parallel \approx 0$, and in the perpendicular direction they are constantly fluctuating from 0 to maximum (time-of-flight background). Therefore, we took an average of events, being left and right of the corresponding H_2 or D_2 time-of-flight peak, and we subtracted this from the data (although the difference between the left and right sides of the time-of-flight peaks was only $\pm$ 0.3%).

III. RESULTS AND DISCUSSION

One possible source of errors in this experiment is the dissociation of D_2^+, which leads to a D^+ ion that has the same time of flight as H_2^+ and also different detection efficiency from that of D_2^+ (≈3% [29]). These problems can be solved by normalization of the *ee* process of the measured H_2^+ ions to the D_2^+ ions. Furthermore, to avoid the possible problem of regions of reduced detection efficiency on the detector, we changed the position of the detector and measured the H_2^+ and D_2^+ ion spots at different positions on our detector. To suppress the background from dissociating D^+ and also H_2^+ from the residual gas and to clean the spectra, we analyze only events with positive momentum in the jet direction (y) without

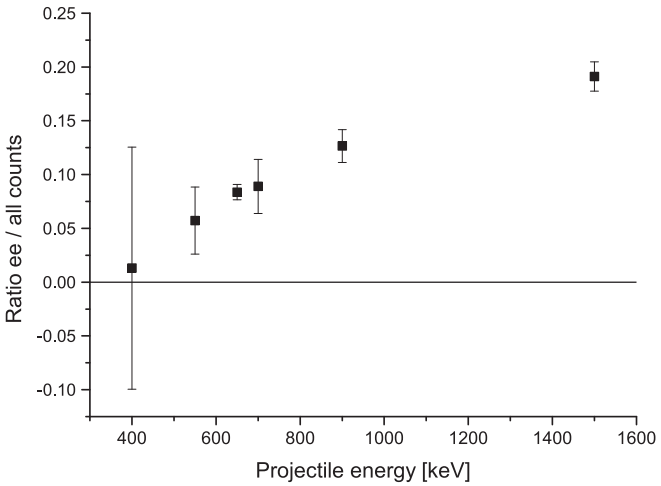

FIG. 3. Ratio of the *ee* process to all counts in mutual projectile and target ionization in $He^+ + H_2$ collisions depending on the projectile energy.

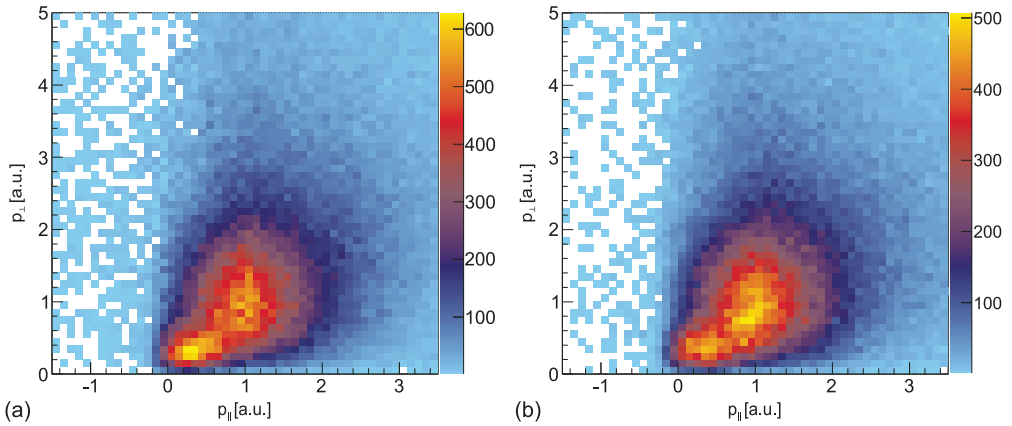

FIG. 4. (Color online) Recoil ion momenta transverse and longitudinal to the incident beam direction for mutual projectile and target ionization for 650 keV He^+ impact onto H_2 (a) and D_2 (b).

loss of generality. In this way, we can completely separate the signal of H_2^+ and D^+.

For the main results of this paper, we choose He^+ projectiles with an energy of 650 keV (162.5 keV/u) colliding with H_2 and D_2. This projectile energy had to be tuned in a way that both processes *ee* and *ne* can be clearly resolved. The *ne* process dominates at smaller projectile energies, while the *ee* process is dominant at higher energies. The ratio of both processes for H_2^+ depending on the projectile energy can be seen in Figs. 2 and 3.

The projectile energy dependence of the *ee* process is shown in Fig. 3. In the H_2^+ doubly differential cross sections, a circle of 0.35 a.u. radius around $p_\parallel = 0.35$ a.u. and $p_\perp = 0.35$ a.u. (circle in Fig. 2) was selected which characterizes the *ee* part of all counts in these spectra. The ratio of this part to all counts was plotted and shows an expected rise of the *ee* process depending on the projectile energy.

After determining the *ee* to *ne* ratio for different projectile energies, we chose 650 keV for our comparison of H_2 versus D_2, because both processes are similarly intense at this energy. Both molecules are separated in time of flight as well as in position on our detector. The recoil ion momenta perpendicular and parallel to the projectile beam direction are plotted in Fig. 4. H_2 is shown on the left, D_2 on the right. In the region of small momentum transfers ($p_\parallel < 0.5$ a.u. and $p_\perp < 1$ a.u.), both spectra show a maximum which corresponds to the *ee* process. The second maximum at larger total momenta corresponds to the *ne* process.

For a more detailed comparison, the longitudinal and transverse momenta of both isotopes are presented separately in Fig. 5. The data have been normalized to the integral (not peak maximum). In both directions, the momentum distributions are almost identical in shape. The size of the statistical error bars is smaller than the points.

Figure 6 shows the ratio of H_2 to D_2 for the transverse (a) and the longitudinal (b) momentum. Small deviations up to 5% fluctuate around 0. Linear fits yield an intercept value of -0.0077 ± 0.0047 and a slope of -0.0049 ± 0.0024 for the case of transverse momentum and an intercept of 0.0065 ± 0.0058 and a slope of -0.0065 ± 0.0039 for the case of longitudinal momentum. These small numbers provide a good indication of the diminutiveness of any deviation from the expectations from standard scattering theory. Most importantly, however, the observed deviations from unity are

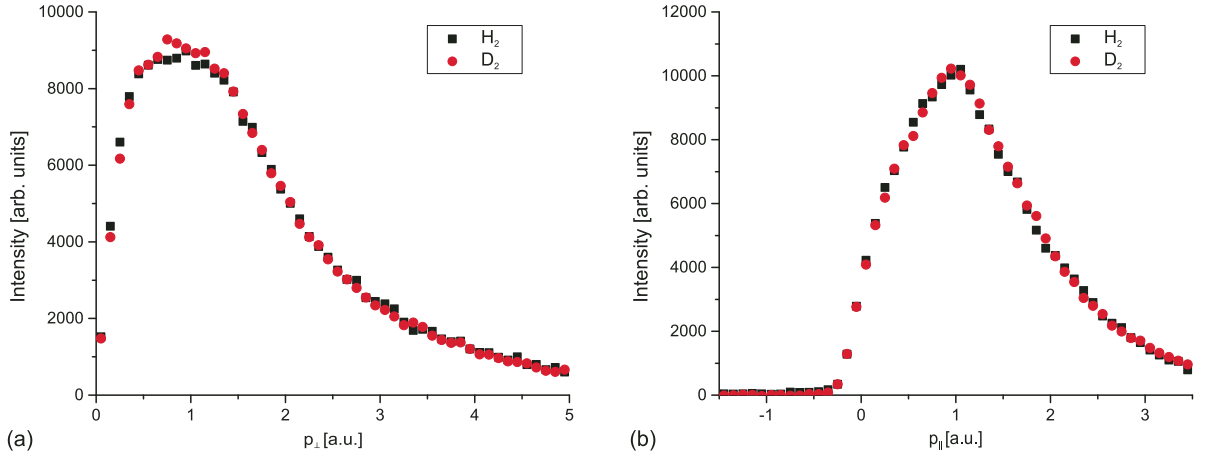

FIG. 5. (Color online) Longitudinal and transverse momenta of H_2^+ and D_2^+ for mutual projectile and target ionization by 650 keV He^+ impact normalized to their integral. The H_2 data points are shown as black squares and the D_2 data points as red circles. The data are projections of the data shown in Fig. 4 onto the horizontal or vertical axis.

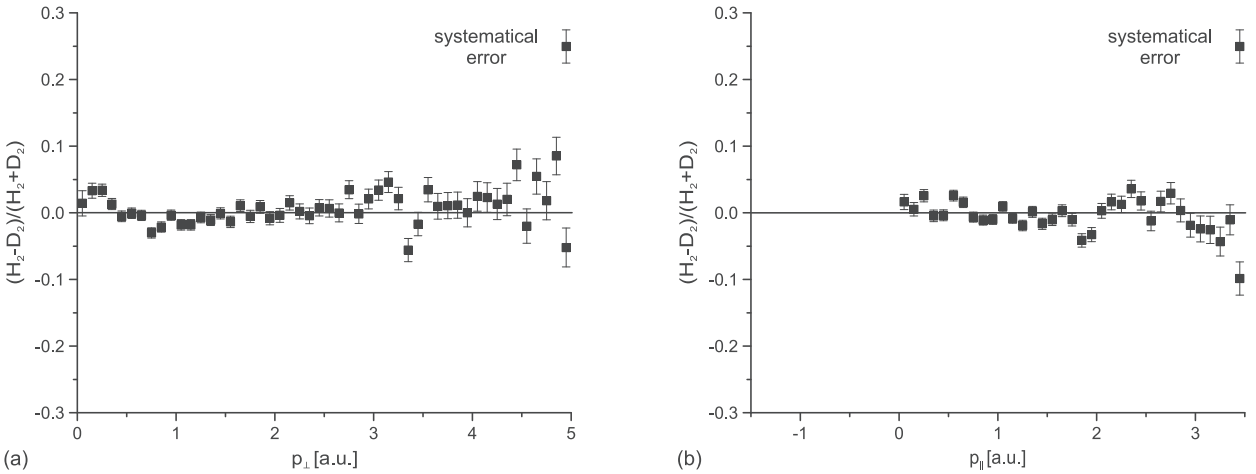

FIG. 6. Normalized differences of the H_2^+ and D_2^+ ions [i.e., $(\sigma_{H_2} - \sigma_{D_2})/(\sigma_{H_2} + \sigma_{D_2})$, results from Fig. 5]. In the case of parallel momentum, events below 0 a.u. are only background and have no physical meaning, therefore they are not shown.

far smaller than the 30% deviation reported for electron or neutron impact [3–6]. As outlined in the Introduction, an isotope effect on electron scattering of 30% would alter the *ne* but not the *ee* contribution. No such effect is observed in our data, in full agreement with the expectation of standard scattering theories.

IV. CONCLUSIONS

The goal of the present measurement was to search for isotope differences in the ionization dynamics in a heavy particle collision with H_2 and D_2. This search is motivated by recent reports on unexpected and so far unexplained isotope differences in the elastic scattering of electrons and neutrons [3–6] of up to 30%. We have investigated electron loss which for one channel (*ne*) can be thought of as a scattering of a quasifree electron at the target nucleus (H_2, D_2), while a second channel (*ee*) provides an independent *in situ* normalization. In contrast to the experimental findings of Cooper *et al*., the present experimental results do not exhibit any significant differences above 5% between the H_2 and D_2 targets. This "null" result is in line with the expectation from all standard scattering theories. A possible reason for the opposite conclusion drawn from our experiment as compared to the surprising results of the electron and neutron scattering is that the momentum transfers are in different regimes: Cooper *et al*. [3] used a momentum transfer q of 19.7 a.u., while in our experiment only momentum transfers of up to 5 a.u. were measured. So a rather different momentum transfer region is probed in this case. At the end of our momentum distribution in Fig. 6, we can see a tendency of an increasing normalized difference for perpendicular momenta and a decreasing normalized difference for parallel momenta. This could be a suggestion of the reported isotope effect at higher momentum transfers, but experiments that enable these higher momentum transfers are needed to explore this possible momentum transfer dependency, as the observed effect could either depend on the momentum transfer or occur only at higher momentum transfers. Chatzidimitriou-Dreismann suggests an increase of the anomaly with increasing momentum transfer [4–6,11]. For further investigation of this question, we plan to perform measurements with higher momentum transfers, but these cannot be reached with our Van de Graaff accelerator; a storage ring is needed instead. For the sum of electron energies in the projectile frame, we can use here the approximation $\sum_{i=1,2} E^p_{\mathrm{kin},e_i} \approx p_{\parallel,\mathrm{rec}} v_p =$ 3.5 a.u. $\times$ 2.55 a.u. $=$ 8.93 a.u. $\approx$ 243 eV [19]. Although the electron energies are not presented in this paper, we consider only electrons below 243 eV due to 3.5 a.u. maximum longitudinal recoil ion momentum.

ACKNOWLEDGMENTS

This work was supported by the DFG and Roentdek Handels GmbH. We acknowledge enlightening discussions with C. A. Chatzidimitriou-Dreismann.

[1] J. T. Muckerman, J. Chem. Phys. **54**, 1155 (1971).
[2] M. J. Berry, J. Chem. Phys. **59**, 6229 (1973).
[3] G. Cooper, A. P. Hitchcock, and C. A. Chatzidimitriou-Dreismann, Phys. Rev. Lett. **100**, 043204 (2008).
[4] C. A. Chatzidimitriou-Dreismann, T. A. Redah, R. M. F. Streffer, and J. Mayers, Phys. Rev. Lett. **79**, 2839 (1997).
[5] C. A. Chatzidimitriou-Dreismann, M. Vos, C. Kleiner, and T. Abdul-Redah, Phys. Rev. Lett. **91**, 057403 (2003).
[6] C. A. Chatzidimitriou-Dreismann, T. Abdul-Redah, and M. Krzystyniak, Phys. Rev. B **72**, 054123 (2005).
[7] N. I. Gidopoulos, Phys. Rev. B **71**, 054106 (2005).
[8] G. F. Reiter and P. M. Platzman, Phys. Rev. B **71**, 054107 (2005).
[9] E. B. Karlsson and S. W. Lovesey, Phys. Rev. A **61**, 062714 (2000).
[10] E. B. Karlsson and S. W. Lovesey, Phys. Scr. **65**, 112 (2002).
[11] C. A. Chatzidimitriou-Dreismann, Laser Phys. **15**, 780 (2005).
[12] R. Moreh, Nucl. Instrum. Methods Phys. Res. B **279**, 49 (2012).

[13] R. Dörner, V. Mergel, R. Ali, U. Buck, C. L. Cocke, K. Froschauer, O. Jagutzki, S. Lencinas, W. E. Meyerhof, S. Nüttgens, R. E. Olson, H. Schmidt-Böcking, L. Spielberger, K. Tökesi, J. Ullrich, M. Unverzagt, and W. Wu, Phys. Rev. Lett. **72**, 3166 (1994).

[14] E. C. Montenegro, W. S. Melo, W. E. Meyerhof, and A. G. de Pinho, Phys. Rev. Lett. **69**, 3033 (1992).

[15] E. C. Montenegro and W. E. Meyerhof, Phys. Rev. A **46**, 5506 (1992).

[16] H. Kollmus, R. Moshammer, R. E. Olson, S. Hagmann, M. Schulz, and J. Ullrich, Phys. Rev. Lett. **88**, 103202 (2002).

[17] T. Ferger, D. Fischer, M. Schulz, R. Moshammer, A. B. Voitkiv, B. Najjari, and J. Ullrich, Phys. Rev. A **72**, 062709 (2005).

[18] X. Wang, K. Schneider, A. Kelkar, M. Schulz, B. Najjari, A. Voitkiv, M. Gundmundsson, M. Grieser, C. Krantz, M. Lestinsky, A. Wolf, S. Hagmann, R. Moshammer, J. Ullrich, and D. Fischer, Phys. Rev. A **84**, 022707 (2011).

[19] R. Dörner, V. Mergel, O. Jagutzki, L. Spielberger, J. Ullrich, R. Moshammer, and H. Schmidt-Böcking, Phys. Rep. **330**, 95 (2000).

[20] J. Ullrich, R. Moshammer, A. Dorn, R. Dörner, L. Ph. H. Schmidt, and H. Schmidt-Böcking, Rep. Prog. Phys. **66**, 1463 (2003).

[21] T. Jahnke, Th. Weber, T. Osipov, A. L. Landers, O. Jagutzki, L. Ph. H. Schmidt, C. L. Cocke, M. H. Prior, H. Schmidt-Böcking, and R. Dörner, J. Electron. Spectrosc. Relat. Phenom. **141**, 229 (2004).

[22] R. Dörner, V. Mergel, R. Ali, U. Buck, C. L. Cocke, K. Froschauer, O. Jagutzki, S. Lencinas, W. E. Meyerhof, S. Nüttgens, R. E. Olson, H. Schmidt-Böcking, L. Spielberger, K. Tökesi, J. Ullrich, M. Unverzagt, and W. Wu, Nucl. Instrum. Methods B **98**, 367 (1995).

[23] R. Dörner, V. Mergel, L. Spielberger, O. Jagutzki, S. Nüttgens, M. Unverzagt, H. Schmidt-Böcking, J. Ullrich, R. E. Olson, K. Tökesi, W. E. Meyerhof, W. Wu, and C. L. Cocke, Nucl. Instrum. Methods B **99**, 111 (1995).

[24] W. Wu, K. L. Wong, R. Ali, C. Y. Chen, C. L. Cocke, V. Frohne, J. P. Giese, M. Raphaelian, B. Walch, R. Dörner, V. Mergel, H. Schmidt-Böcking, and W. E. Meyerhof, Phys. Rev. Lett. **72**, 3170 (1994).

[25] W. Wu, K. L. Wong, E. C. Montenegro, R. Ali, C. Y. Chen, C. L. Cocke, R. Dörner, V. Frohne, J. P. Giese, V. Mergel, W. E. Meyerhof, M. Raphaelian, H. Schmidt-Böcking, and B. Walch, Phys. Rev. A **55**, 2771 (1997).

[26] See http://www.roentdek.com for details on the detectors.

[27] O. Jagutzki, V. Mergel, K. Ullmann-Pfleger, L. Spielberger, U. Spillmann, R. Dörner, and H. Schmidt-Böcking, Nucl. Instrum. Methods Phys. Res. A **477**, 244 (2002).

[28] M. S. Schöffler, T. Jahnke, J. Titze, N. Petridis, K. Cole, L. Ph. H. Schmidt, A. Czasch, O. Jagutzki, J. B. Williams, C. L. Cocke, T. Osipov, S. Lee, M. H. Prior, A. Belkacem, A. L. Landers, H. Schmidt-Böcking, R. Dörner, and Th. Weber, New. J. Phys. **13**, 095013 (2011).

[29] M. Krems, J. Zirbel, M. Thomason, and R. D. DuBois, Rev. Sci. Instrum. **76**, 093305 (2005).